ACS APPLIED MATERIALS & INTERFACES

Research Article

www.acsami.org

Preparation of TiO_2 Nanoparticles Coated with Ionic Liquids: A Supramolecular Approach

Izabelle M. Gindri,[†] Clarissa P. Frizzo,*[,‡] Caroline R. Bender,[‡] Aniele Z. Tier,[‡] Marcos A. P. Martins,[‡] Marcos A. Villetti,[‡] Giovanna Machado,[§] Lucas C. Rodriguez,[†] and Danieli C. Rodrigues[†]

[†]Department of Bioengineering, The University of Texas at Dallas, Richardson, Texas 75080, United States

[‡]Department of Chemistry, Federal University of Santa Maria, Santa Maria, Rio Grande do Sul 97105-900, Brazil

[§]Centro de Tecnologias Estratégicas do Nordeste (CETENE), Microscopia Eletrônica e Nanotecnologia, Recife, Pernambuco 50740540, Brazil

Supporting Information

ABSTRACT: Coated TiO_2 nanoparticles by dicationic imidazolium-based ionic liquids (ILs) were prepared and studied by differential scanning calorimetry (DSC), dynamic light scattering (DLS), transmission electron microscopy (TEM), powder X-ray diffraction (XRD), and scanning electron microscopy (SEM). Three ILs with different hydrophobicity degrees and structural characteristics were used (IL-1, IL-2, and IL-3). The interaction between IL molecules and the TiO_2 surface was analyzed in both solid state and in solution. The physical and chemical properties of coated nanoparticles (TiO_2 + IL-1, TiO_2 + IL-2, and TiO_2 + IL-3) were compared to pure materials (TiO_2, IL-1, IL-2, and IL-3) in order to evaluate the interaction between both components. Thermal behavior, diffraction pattern, and morphologic characteristics were evaluated in the solid state. It was observed that all mixtures (TiO_2 + IL) showed different behavior from that detected for pure substances, which is an evidence of film formation. DLS experiments were conducted to determine film thickness on the TiO_2 surface comparing the size (hydrodynamic radius, R_h) of pure TiO_2 with coated nanoparticles (TiO_2 + IL). Results showed the thickness of the film increased with hydrophobicity of the IL compound. TEM images support this observation. Finally, X-ray diffraction patterns showed that, in coated samples, no structural changes in TiO_2 diffraction peaks were observed, which is related to the maintenance of the crystalline structure. On the contrary, ILs showed different diffraction patterns, which confirms the hypothesis of interactions happening between IL and the TiO_2 nanoparticles surface.

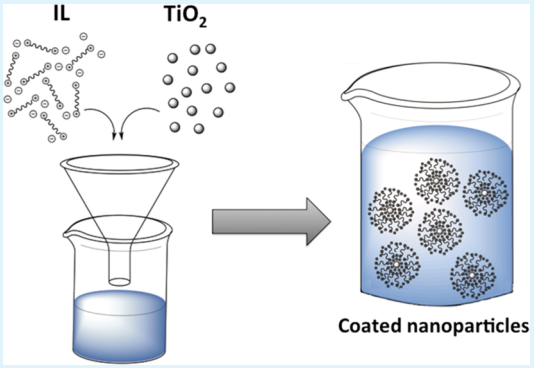

KEYWORDS: *ionic liquids, TiO_2, nanoparticles, film, coating, interaction*

INTRODUCTION

Titanium dioxide is one of the most technologically important oxide materials. It has been broadly studied due to its wide range of applications including: catalysis, solar cells, sensors, pigments, corrosion protection, biomaterials, and optical coatings.[1−9] The electronic structure of TiO_2 plays a key role in the interaction mode between the oxide surface and other materials. Chemisorption on the TiO_2 surface is strongly affected by the ionic nature of the crystal. The crystal structure of TiO_2 shows each titanium (Ti) atom surrounded by six oxygen (O) atoms. The characteristic bonds between Ti and O include a high degree of ionicity, which has been reported to be approximately 70%.[10] Ti cations on the surface of TiO_2 are coordinately unsaturated and act as Lewis acids (electron pair acceptor) and may interact with electron donors. On the other hand, oxygen atoms are basic sites and interact with electron acceptors such as protons (H^+) creating bridging hydroxyls (OH groups).[10]

Ionic liquids (ILs) are molten salts, which possess a combination of excellent properties such as (a) nonvolatility, (b) thermo-oxidative stability, (c) high ionic conductivity, (d) a wide electrochemical window, (e) miscibility with organic compounds, and (f) being inert to air and water. Additionally, the properties of ILs can be finely tuned; varying their structure can have an influence on their polar and dispersive interactions. There is a wide range of applications for ILs in different fields of science such as being used as solvents,[11] in catalysis,[11] electrochemistry,[12] and corrosion protection,[13] and ultimately in the preparation of nanoparticle dispersions.[9]

Given the structure of the TiO_2, it is possible to infer that materials such as ionic liquids (ILs), which are composed of cations and anions, can interact with both sites present in the surface of TiO_2. However, a few studies showed that TiO_2 has a

Received: April 14, 2014
Accepted: June 16, 2014
Published: June 16, 2014

ACS Publications © 2014 American Chemical Society

dx.doi.org/10.1021/am5022107 | ACS Appl. Mater. Interfaces 2014, 6, 11536−11543

Table 1. Numbering and Structure of Synthesized ILs

Compound	IL structure
IL-1	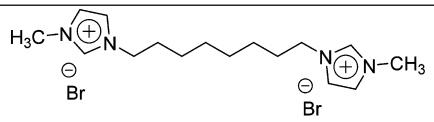
IL-2	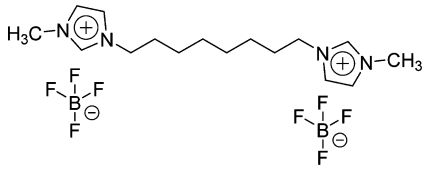
IL-3	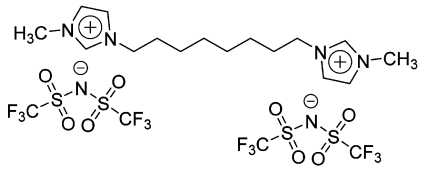

higher affinity for anionic moieties. Results from ionic liquids and amino acid adsorption and also with aqueous sodium chloride solution, for example, show a predominance of anions adsorption on TiO_2 surfaces.[14−17] The interaction between ILs and the surface of titanium and its alloys has been previously investigated in applications involving high temperature and lubrication.[13,18−20] There is data from both experimental techniques and advanced theoretical methods that give evidence of the interaction between charged particles on titanium surfaces.[15,17,21−27] In experiments with nanoparticles of TiO_2, Wang et al. studied the interfacial structure between 1-butyl-3-methyl-imidazolium hexafluorophosphate [BMIM]-[PF_6] and the rutile (110) surface by classical molecular dynamics simulation.[17] The simulation results showed several layers formed on the interfacial region, especially for the anions. A well-ordered double layered ionic structure was also observed in the interfacial region where ions are self-organized into alternate double ionic layers. The cations were found to organize themselves in parallel alignment with respect to the anions on the TiO_2 surface, with an obvious elongation of the side chains.[17,23,28,29]

The dispersibility of different commercial TiO_2 nanoparticles in ILs was evaluated by Ulbricht and Wittmar.[9] In that study, they analyzed the interaction of TiO_2 and IL through dynamic light scattering and rheology. It was concluded that colloidal stabilities of the resulting dispersions were strongly influenced by particle characteristics such as aggregation level, mean particle size, and surface functionality. Other important factors observed were the influence of the structure and hydrophilicity of the IL investigated. It was observed that particle size tends to increase with increasing anion hydrophobicity.[9] The association between TiO_2 nanoparticles and ILs have been investigated by different techniques and proved to increase the performances of lithium batteries and solar cells.[8,18]

The goal of this research is to investigate the influence of IL structure on film formation on the surface of TiO_2 nanoparticles using a molecular to supramolecular characterization approach of the interactions between IL and TiO_2 nanoparticles. Dicationic imidazolium-based ionic liquids with different anions were evaluated (Table 1). The effect of IL hydrophobicity degree on film formation on the surface of the nanoparticles was also determined. Film characterization was carried out by calorimetric and spectroscopic techniques using differential scanning calorimetry (DSC), dynamic light scattering (DLS), transmission electron microscopy (TEM), scanning electron microscopy (SEM), and powder X-ray diffraction (XRD). The comprehension of the interactions between these materials is unquestionably of large technological and scientific interest for the development of innovative technologies for surface protection of several materials or in energy devices.

EXPERIMENTAL SECTION

Materials. The reactants 1-methylimidazole, 1,8-dibromooctane, sodium tetrafluoroborate, bis(trifluoromethane)sulfonamide lithium salt, and TiO_2 nanoparticles and solvents acetonitrile (HPLC), ethyl ether (HPLC), ethyl acetate, and ethanol were purchased from Sigma-Aldrich (St Louis, MO, USA) and Tedia (Rio de Janeiro, RJ, BR), respectively; all chemicals products were of high-grade purity and were used without purification.

IL Synthesis and Characterization. The ILs were synthesized in accordance with methodologies previously developed in our laboratories[30] and with that described by Shirota et al.[31] The structures of all of the products were confirmed by NMR and mass spectra. Electrospray ionization mass spectra (ESI-MS) were acquired with Agilent Technologies 6460 Triple quadrupole 6460 (LC/MS-MS) (Santa Clara, CA, USA), operated in the positive-ion mode. The gas temperature was 300 °C; the flow of the drying gas was 5 L/min, and the nebulizer was at 45 psi. The voltage of the capillary was 3500 V, and the fragmentor was 0 V. The ionic liquid solutions in H_2O were introduced at a 5 $\mu L \cdot min^{-1}$ flow rate. Nitrogen was used as nebulization gas and argon as collision gas. Molecular ions were detected using positive mode, where m/z ratio is given for one dication and one anion. NMR ^1H and ^{13}C NMR spectra were recorded on a Bruker DPX 400 (Billerica, MA, USA) (^1H at 400.13 MHz and ^{13}C at 100.32 MHz) and in 5 mm sample tubes at 298 K (digital resolution of ±0.01 ppm) in DMSO-d_6 using TMS as internal reference. The NMR peak of DMSO (δ = 2.50) was used as the reference in determining the chemical shifts of ^1H in ILs. Elemental analyses were performed on a PerkinElmer CHN 2400 elemental analyzer. Water content in the

Table 2. Thermal Behavior of Pure IL and Mixture of IL and TiO_2[a]

	IL-1		IL-2		IL-3	
thermal analysis	pure	IL-1 + TiO_2	pure	IL-2 + TiO_2	pure	IL-3 + TiO_2
MP_1(°C)[b]	70.2 (±1.0)	67.8 (±0.6)	72.4 (±1.0)	62.3 (±3.1)	–[j]	−29.8[c]
MP_2(°C)[d]	–[j]	213.1 (±5.1)	–[j]	–[j]	–[j]	–[j]
$\Delta H°_{f1}$ (kJ/mol)[e]	34.1 (±7.6)	38.1 (±5.8)	22.9 (±2.6)	32.3 (±2.9)	–[j]	1.06
$\Delta H°_{f2}$ (kJ/mol)[f]	–[j]	31.7 (±11.8)	–[j]	–[j]	–[j]	–[j]
T_g (°C)[g]	–[j]	–[j]	39.5 (±1.8)	–[j]	−61.8 (±0.8)	−61.9 (±1.2)
T_{d1} (°C)[h]	307.5	310.0	346.8	343.8	473	463
T_{d2} (°C)[i]	–[j]	372.9	455.8	455.8	–[j]	–[j]

[a]All DSC data are given as average and SD of three measurements. [b]First melting point. [c]Melting point observed once. [d]Second melting point. [e]Fusion entalphy of first melting point. [f]Fusion entalphy of second melting point. [g]Glass transition temperature. [h]First step decomposition temperature. [i]Second step decomposition temperature. [j]No thermal event detected.

ILs was determined by Karl Fisher titration (Titrando 836, Metrohm, Brazil). It was found that less than 0.5 wt % water was contained in all the ILs studied. The content of bromide was determined by ion chromatography (IC) using a model 850 Professional IC (Metrohm, Herisau, Switzerland) equipped with an 858 Professional Sample Processor and conductivity detector. 0.26 and 0.002 mol·kg^{-1} of the impurity were observed in LI-2 and LI-3, respectively. The spectral data is available in the Supporting Information.

Nanoparticle Coating. The interaction between different ILs with TiO_2 nanoparticles was evaluated with experiments performed in both solution (dynamic light scattering) and solid state (differential scanning calorimetry, X-ray diffraction, and scanning electron microscopy). In the first step, solutions of pure compounds (IL-1, IL-2, IL-3, and TiO_2 nanoparticles) and the coated nanoparticle of TiO_2 with each IL (TiO_2 + IL-1, TiO_2 + IL-2, TiO_2 + IL-3) were prepared. For simplicity, coated TiO_2 nanoparticles will be referred to as a mixture of TiO_2 + IL, through the remainder of the text. The solid state samples of TiO_2 + IL were obtained from solvent evaporation from solutions. Both solutions and solid state samples were prepared as follows.

Preparation of TiO_2 Nanoparticles Solution. Ethanolic solutions of TiO_2 nanoparticles were prepared by weighing the material in a volumetric balloon using an analytical balance (Marte AL 500, Sao Paulo, SP, Brazil). The volume was completed with a mixture of ethanol/water 1:1.

Preparation of IL Solutions. Ethanolic solutions of each IL (IL-1, IL-2, and IL-3) were prepared by weighing the amount of IL in a volumetric balloon using an analytical balance (Marte AL 500, Sao Paulo, SP, Brazil). The volume was completed with a mixture of ethanol/water 1:1.

Preparation of Solutions Containing the Mixture of TiO_2 + IL. Ethanolic solutions of an equimolar ratio between IL and TiO_2 were prepared by weighing both compounds in a volumetric balloon using an analytical balance (Marte AL 500, Sao Paulo, SP, Brazil). The volume was completed with a mixture of ethanol/water 1:1.

Solid State Samples. The equal molar ratios of ILs/TiO_2 were weighted in a crystallization plate and diluted in 5 mL of 50% ethanol/water solution (4 mol·L^{-1} of IL-1 and IL-2; 2 mol·L^{-1} of IL-3). The solutions were evaporated at room temperature under magnetic stirring for 30 min. The samples were then stored in the oven at 40 °C for 24 h. Subsequently, the samples were maintained under vacuum for 5 days at 40 °C, in order to remove any residual solvent. The resultant solid powders were used to perform DSC, powder X-ray diffraction analysis, and SEM.

Differential Scanning Calorimetry (DSC). Solid samples of pure TiO_2 nanoparticles, pure IL (IL-1, IL-2, and IL-3), and the mixture of TiO_2 + IL (TiO_2 + IL-1, TiO_2 + IL-2, TiO_2 + IL-3) were analyzed by DSC. The DSC experiments were performed using a MDSC Q2000 (T-zeroTM DSC technology, TA Instruments Inc., New Castle, DE, USA). Dry high purity (99.999%) nitrogen gas was used as the purge gas (50 mL min^{-1}). The instrument was initially calibrated using melting indium (156.60 °C). The heat capacity calibration was done by running a standard sapphire (α-Al_2O_3). The heating rate used for all the samples was 10 °C min^{-1}. Each IL was subjected to three cycles of heating and cooling in the temperature range from −80 to 250 °C for IL-1 and −80 to 300 °C for IL-2 and IL-3. The masses of the reference and sample pans with lids were measured and shown to be 51 ± 0.02 mg. Samples were crimped into hermetic aluminum pans with lids and weighed in a precision balance.

Dynamic Light Scattering (DLS). The solutions of pure TiO_2 nanoparticles, pure ILs (IL-1, IL-2 and IL-3), and the mixtures of TiO_2 + IL-1, TiO_2 + IL-2, and TiO_2 + IL-3, prepared as described previously, were analyzed. To obtain the thickness of the film formed on the TiO_2 surface, the hydrodynamic radius (R_h) obtained for pure TiO_2 nanoparticles was subtracted from the R_h values obtained for each mixture of TiO_2 + IL. The dynamic light scattering measurements (DLS) were performed at 298.15 K on a Zetasizer Nano ZS light scattering apparatus (Malvern Instruments, Malvern, UK, USA) with a He−Ne laser (5.0 mW). The solutions were filtered directly into the quartz cell using a membrane filter of 0.45 μm pore size. Three repeated measurements were performed for each sample, and the reproducibility of aggregate size was ±3%.

Transmission Electron Microscopy (TEM). The samples of pure TiO_2 nanoparticles and the mixture of TiO_2 + IL (TiO_2 + IL-1, TiO_2 + IL-2, TiO_2 + IL-3) were analyzed by TEM (Tecnai G2-12 Spirit BioTwin, FEI Company). The images were examined using a TEM at 120 kV. The samples were prepared by dispersion of the solutions at room temperature on a carbon-coated copper grid.

Scanning Electron Microscopy (SEM). The solid samples of pure TiO_2 nanoparticles, pure IL-1 and IL-2, and the mixture of TiO_2 + IL (TiO_2 + IL-1 and TiO_2 + IL-2) were analyzed by SEM (JEOL, JSM6360LV, Akishima, Japan). It was not possible to analyze the pure IL-3 and the mixture of TiO_2 + IL-3 due the physical characteristics of samples. Samples were gold coated for SEM analysis.

Powder X-ray Diffraction. Solid samples of pure TiO_2 nanoparticles, pure IL-1 and IL-2, and the mixture of TiO_2 + IL (TiO_2 + IL-1 and TiO_2 + IL-2) were analyzed by powder X-ray diffraction. It was not possible to analyze the pure IL-3 and the mixture of TiO_2 + IL-3 due the physical characteristics of the samples. The patterns of X-ray diffraction were recorded on a Rigaku Miniflex 300 powder diffractometer connected to a Goniometer (30 kV, 10 mA). Cu Kα radiation monochromatized by a bent graphite crystal was used (λ = 1.54051 Å). Patterns were collected in step scan mode with a step of 0.01 and counting time of 0.5 s in the angular range of 2° to 40° with θ−2θ configuration. The powder was manually pressed inside the standard grooved sample holder. All spectra were collected in air at room temperature.

RESULTS AND DISCUSSION

Experiments were conducted with imidazole derived-ILs with the anions Br^-, BF_4^-, and NTf_2^- as contra-ions in order to evaluate the affinity of ILs with the TiO_2 surface. The structure of synthesized ILs is illustrated in Table 1. TiO_2 nanoparticles (~21 nm) were used for this investigation instead of bulk material to allow for a better understanding of the interactions

Table 3. DLS Data for TiO_2 Nanoparticles and Mixtures of TiO_2 and IL[a]

DLS	TiO_2	TiO_2 + IL-1	thickness (nm)	TiO_2 + IL-2	thickness (nm)	TiO_2 + IL-3	thickness (nm)
R_{h1} (nm)	0.7 (±0.1)	0.6 (±0.1)	0.1 (±0.2)	0.7 (±0.0)	0.0 (±0.7)	1.2 (±0.0)	0.5 (±1.5)
R_{h2} (nm)	337.8 (±48.5)	450.7 (±25.2)	112.9 (±54.7)	497.2 (±22.4)	159.4 (±53.4)	1248.2 (±141.8)	910.4 (±106.0)

[a]Average values and standard deviations (±SD) are indicated for each parameter measured. h1: relaxation mode 1; h2: relaxation mode 2.

between the selected ILs with the Ti oxide film (TiO_2). The use of particles allowed for the investigation of the properties of the TiO_2–IL compounds employing techniques such as dynamic light scattering. DLS provided information about particle growth with the addition of IL layers on the surface.[32] Other techniques used for this preliminary evaluation included transmission electron microscopy (TEM), differential scanning calorimetry, powder X-ray diffraction, and scanning electron microscopy.

Differential Scanning Calorimetry (DSC). Both the melting point and the enthalpy of fusion of these complex mixtures tend to change because of several contributing factors such as, different molecular arrangements in the lattice, intermolecular interactions, and conformational flexibility due to differences between the mixture and starting materials.[33−37] The thermal behaviors of TiO_2 nanoparticles, pure IL, and the mixture of TiO_2 and the different ILs synthesized were evaluated. The thermal behavior of the samples analyzed is summarized in Table 2.

The results show that TiO_2 nanoparticles do not have any thermal event in a cycle of heating and cooling (range of −80 to 400 °C). This is a result of the high melting point of the metal oxide TiO_2, which is approximately 1845 °C. On the contrary, the analysis of IL compounds revealed both melting point (IL-1 and IL-2) and glass transition (IL-2 and IL-3). These transitions were compared to the values obtained for the different mixtures of TiO_2 + IL (IL-1, IL-2, and IL-3). Comparing the results between pure IL-1 and the mixture of TiO_2 + IL-1, the presence of two melting points in the mixture of TiO_2 + IL-1 can be observed. The first transition (67.8 °C) has the same temperature as that of the pure IL, and the appearance of a second melting point (213.1 °C) is considered to be an indication that a new crystalline phase was formed, which is probably due to an interaction between TiO_2 nanoparticles and IL-1. The mixture of TiO_2 + IL-2 had a different melting point in comparison to the pure IL. In this case, the temperature decreased about 10.1 °C, which shows that the interaction between both components resulted in a different crystalline arrangement. The enthalpy of fusion of the mixture increased about 9.4 kJ mol^{-1} in relation to the pure IL, which indicates the presence of interactions between TiO_2 and IL-2 in relation to the pure IL. The pure IL-3 demonstrated only glass transition at around −61.8 °C. However, with the addition of TiO_2, a new melting point could be detected from which it can be concluded that the interaction between TiO_2 and IL-3 conferred a more organized structural arrangement. The thermal stabilities for both pure substances and mixtures were also determined. In general, the results showed high thermal stability for both pure compounds and also the mixtures analyzed (>307 °C).

Dynamic Light Scattering (DLS). Dynamic light scattering was used to evaluate the size characteristics of new structures formed by TiO_2 + IL.[9,38−41] Experiments were performed with samples composed of pure TiO_2 nanoparticles in solution and with mixtures of TiO_2 + IL in solution. The results are summarized in Table 3.

The hydrodynamic radius (R_h) of TiO_2 nanoparticles and mixtures of TiO_2 + IL (IL-1, IL-2, and IL-3) was monitored and compared in order to analyze the formation of new organized phases of IL films on TiO_2 nanoparticles surface. Two relaxation modes (R_{h1} and R_{h2}) were detected from the DLS analysis, indicating that all systems are polydisperse. The value from the difference between the size of TiO_2 + IL (IL-1, IL-2, and IL-3) and TiO_2 nanoparticles was used to calculate the IL film thickness formed on TiO_2 surface. The calculated differences in R_h are demonstrated in Figure 1 for the R_{h2} relaxation mode. Comparing the results obtained for TiO_2 nanoparticles and the mixtures of TiO_2 + IL-1, TiO_2 + IL-2, and TiO_2 + IL-3, a small difference between the size of the particles can be observed in the first relaxation mode (R_{h1}). This can be due to the formation of small aggregates as observed for pure IL reported in the literature.[42] The size of the anions can be related to the size of aggregates formed by ILs. The anions with smaller sizes in IL-1 and IL-2 (Br^- and BF_4^-, respectively) showed a small difference in particle size in comparison to TiO_2. However, the larger anion of IL-3 (NTf_2^-) resulted in a larger particle size. In regards to the second relaxation mode, a significant difference was noted between pure TiO_2 nanoparticles and mixtures of TiO_2 + IL (Table 2), which can be related to the formation of alternating layers of cations and anions on the surface of the nanoparticles. An interesting characteristic noted from the DLS results is that film thickness increased with hydrophobicity of the anions (Figure 1), which is in agreement with the trend reported by Ulbricht and Wittmar.[9]

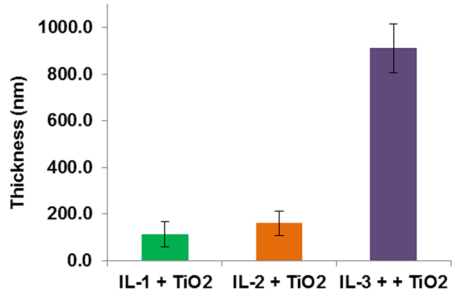

Figure 1. Thickness of IL film of second relaxation mode detected by DLS.

A proposed schematic organization of layers of IL formed on the surface of TiO_2 particles is shown in Figure 2 for the first layers of coordination.

As demonstrated in Figure 2, TiO_2 nanoparticles tend to aggregate. However, while in the presence of IL in solution, these aggregates tend to show even larger size due to the presence of IL layers. Thus, the hypothesis proposed using DLS is also corroborated by TEM observations (Figure 2), from which it is possible to verify film formation on the TiO_2 nanoparticle agglomerates. This aggregation of TiO_2 nanoparticles has the effect of reducing the surface area of nanoparticles available for interactions with IL. Thus, there is

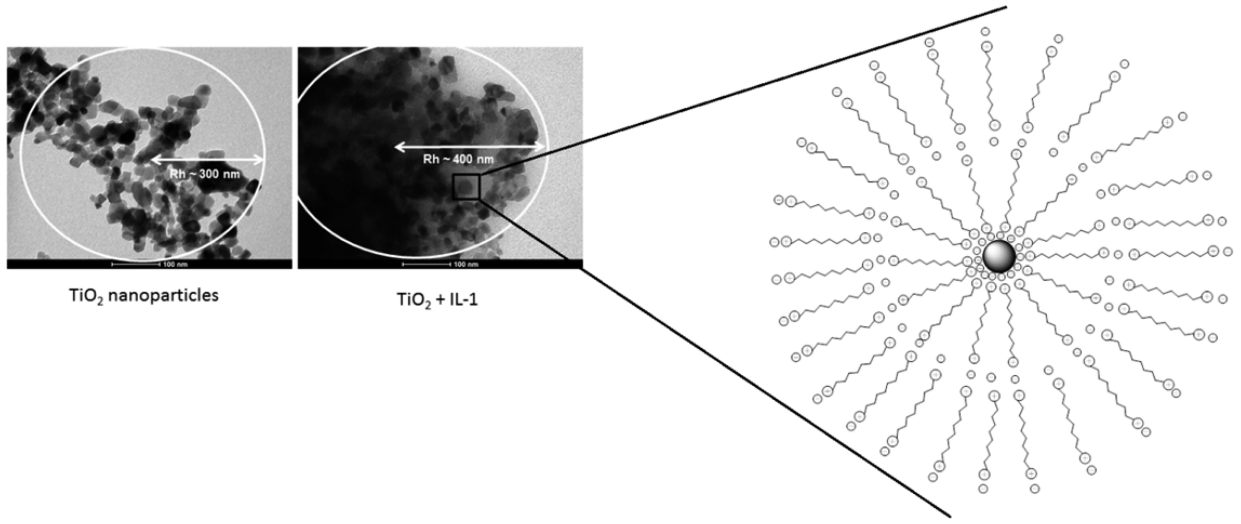

Figure 2. TEM images for TiO_2 nanoparticles and TiO_2 + IL-1 and schematic representation of layers of IL on the surface of nanoparticles.

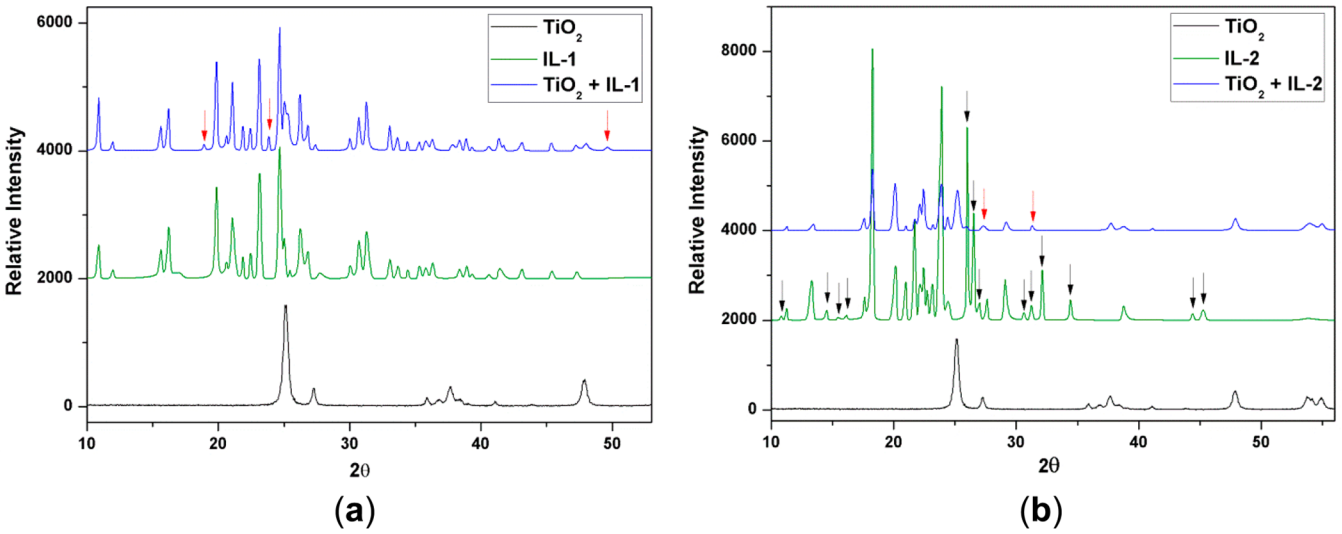

Figure 3. (a) XRD data of pure TiO_2 and IL-1 and the mixture of TiO_2 + IL-1 and (b) XRD data of pure TiO_2 and IL-2 and the mixture of TiO_2 + IL-2.

an excess of IL in the suspension. However, this excess is not sufficient to lead to the dispersion of nanoparticles. Therefore, it is plausible to consider that, besides the first layer represented in Figure 2, there are also successive IL layers adsorbed on the surface of nanoparticle agglomerates.

Powder X-ray Diffraction. Powder X-ray diffraction analysis to evaluate the formation of mixture systems, such as cocrystals and eutectic mixtures, is based on the different diffraction patterns between starting materials and the final mixture.[36,37,43] The interactions between TiO_2 nanoparticles and ILs were observed through diffraction peaks, which indicated the existence of new crystalline phases. The results obtained from powder X-ray diffraction were directly related to the bulk composition of the materials. Therefore, in order to observe changes in the diffraction patterns of the materials in analysis, it was necessary that the internal structure of these materials underwent changes. The comparison among diffraction patterns of pure IL, pure TiO_2 nanoparticles, and the mixtures of TiO_2 + IL is illustrated in Figure 3. Only IL-1 and IL-2 could be analyzed due to the material properties of the final mixture. The spectrum of the TiO_2 + IL-1 mixture (Figure 3a) shows the presence of peaks corresponding to those of pure materials, which indicates the maintanence of most of the crystalline structure of both materials in the mixture. New diffraction peaks can also be observed in the mixture, as indicated by the red narrows in Figure 3a. It is possible to observe that film formation by IL led to a fine packing on the surface of the TiO_2 nanoparticles, similarly to that observed for the pure material. These results are in agreement with those observed by DSC, which demonstrated both the melting point for the pure IL-1 and a new melting point at approximately 213.1 °C in the mixture of TiO_2 + IL-1. The XRD results for the mixtures of TiO_2 + IL-2 showed different characteristics (Figure 3b). The presence of new peaks (red arrows in Figure 3b) and also the absence of peaks (black arrows in Figure 3b), which were characteristics from the pure IL-2, could be observed. This observation supports the hypothesis that the IL changed its packing when absorbed on the surface of the nanoparticles. The reduced intensity of diffraction peaks of TiO_2 for both IL-1 and IL-2 in the mixture spectra confirm that there are layers of ILs deposited under TiO_2 avoiding total infiltration of the X-ray. This observation is also confirmed by

dx.doi.org/10.1021/am5022107 | ACS Appl. Mater. Interfaces 2014, 6, 11536−11543

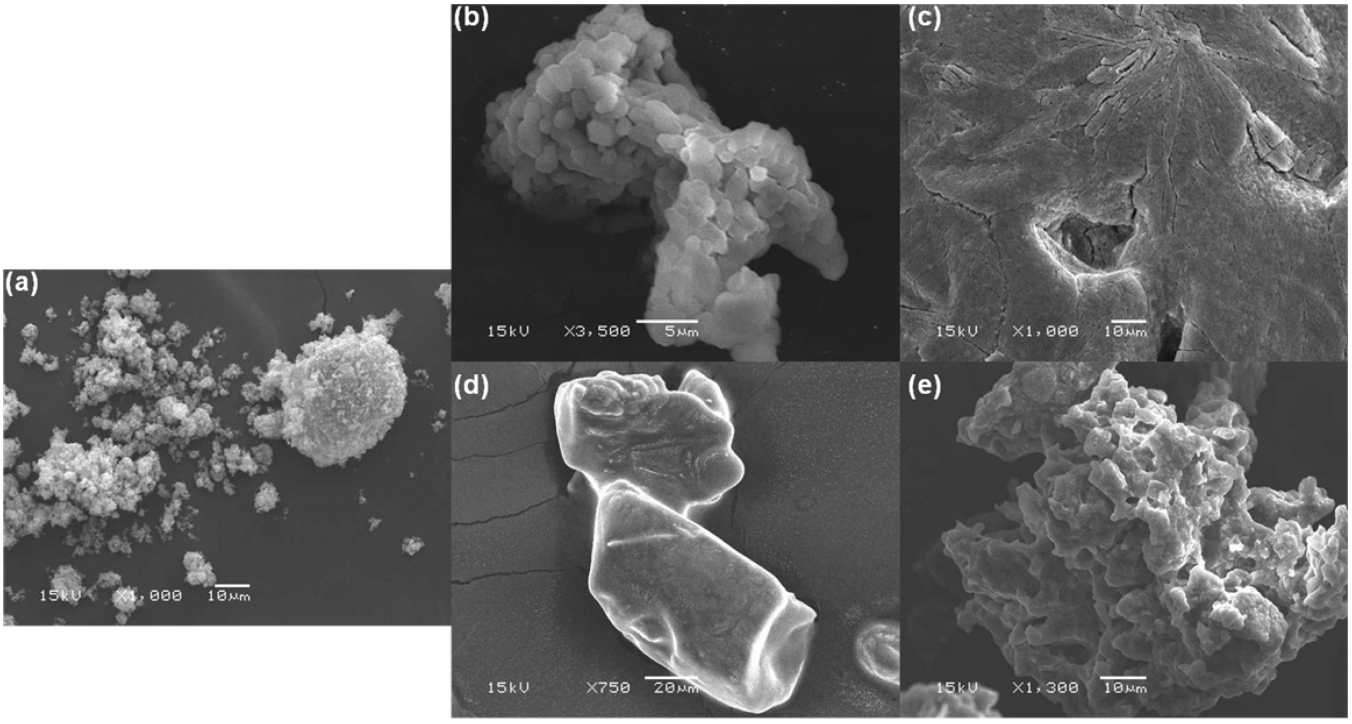

Figure 4. SEM image of (a) TiO_2, (b) IL-1, (c) IL-2, (d) TiO_2 + IL-1, and (e) TiO_2+ IL-2.

the DSC analysis of the mixture, from which a different melting point of the mixture in relation to the pure IL could be observed.

Scanning Electron Microcopy. The SEM analysis provided information on the morphological characteristics emergent from the association between TiO_2 and different IL structures.[44−46] Figure 4 illustrates the morphological structure of pure TiO_2 nanoparticles, IL-2, and IL-3 and the mixture of TiO_2 + IL-1 and TiO_2 + IL-2. Figure 4a shows TiO_2 nanoparticles, which are characterized by small particle size, which tended to form agglomerates. The same behavior was observed for the IL-1, which can be seen to form small aggregates (Figure 4b). On the contrary, the IL-2 was observed to have a more organized structure, with larger crystals formed (Figure 4d). SEM demonstrated that morphological changes occurred when comparing pure materials and the mixtures (TiO_2 + IL-1, Figure 4c; and TiO_2 + IL-2, Figure 4e). Coating TiO_2 nanoparticles with the designed ILs resulted in different structures in relation to pure ILs and TiO_2 particles.

CONCLUSIONS

In this paper, results concerning IL deposition on the surface of TiO_2 nanoparticles are reported. Changes were observed in the thermal and spectroscopic properties of the mixtures of IL and TiO_2 in relation to pure materials, which indicate interactions between these two materials. The structural characteristics of ILs also showed influence on film formation on the surface of TiO_2 nanoparticles. The thickness of the film increased with the increase in IL hydrophobicity, which is conferred by the anionic moiety. The macroscopic features of mixtures obtained by DLS and TEM were also important to evaluate the emergence of film formation in a larger scale. Thus, the results presented indicated the interactions between these two components. These features are valuable for a better rationalization to synthesize ILs for a variety of applications. The influence of hydrophobicity degree and structural changes in the film characteristics can help elucidate the requirements for biological use.

ASSOCIATED CONTENT

Supporting Information

Additional experimental details, ^{1}H NMR spectra, ^{13}C NMR spectra, thermograms, a DLS spectrum, and TEM images. This material is available free of charge via the Internet at http://pubs.acs.org.

AUTHOR INFORMATION

Corresponding Author

*E-mail: clarissa.frizzo@gmail.com.

Author Contributions

The manuscript was written through contributions of all authors. All authors have given approval to the final version of the manuscript.

Notes

The authors declare no competing financial interest.

ACKNOWLEDGMENTS

The authors are thankful for the financial support from the Conselho Nacional de Desenvolvimento Cientifico e Tecnológico (CNPq) (Universal/Proc. 471519/2009, Universal/Proc. 475556/2012-7) and also from the Fundação de Amparo à Pesquisa do Estado do Rio Grande do Sul (FAPERGS) (PRONEX/Proc. 10/0037-8). The fellowships from CNPq (M.A.P.M., C.R.B.) in the fellowships from CNPq, and CAPES (A.Z.T., I.M.G.) are also acknowledged.

REFERENCES

(1) Baghriche, O.; Rtimi, S.; Pulgarin, C.; Sanjines, R.; Kiwi, J. Innovative TiO_2/Cu Nanosurfaces Inactivating Bacteria in the Minute

Range under Low-intensity Actinic Light. *ACS Appl. Mater. Interfaces* **2012**, *4*, 5234−5240.
(2) Spadavecchia, J.; Boujday, S.; Landoulsi, J.; Pradier, C.-M. nPEG-TiO_2 Nanoparticles: A Facile Route to Elaborate Nanostructured Surfaces for Biological Applications. *ACS Appl. Mater. Interfaces* **2011**, *3*, 2637−2642.
(3) Zhao, X.; Wang, G.; Zheng, H.; Lu, Z.; Zhong, Z.; Cheng, X.; Zreiqat, H. Delicate Refinement of Surface Nanotopography by Adjusting TiO_2 Coating Chemical Composition for Enhanced Interfacial Biocompatibility. *ACS Appl. Mater. Interfaces* **2013**, *5*, 8203−8209.
(4) Frandsen, C. J.; Brammer, K. S.; Noh, K.; Johnston, G.; Jin, S. Tantalum Coating on TiO_2 Nanotubes Induces Superior Rate of Matrix Mineralization and Osteofunctionality in Human Osteoblasts. *Mater. Sci. Eng., C* **2014**, *37*, 332−341.
(5) Miyauchi, T.; Yamada, M.; Yamamoto, A.; Iwasa, F.; Suzawa, T.; Kamijo, R.; Baba, K.; Ogawa, T. The Enhanced Characteristics of Osteoblast Adhesion to Photofunctionalized Nanoscale TiO_2 Layers on Biomaterials Surfaces. *Biomaterials* **2010**, *31*, 3827−3839.
(6) Lorenzetti, M.; Biglino, D.; Novak, S.; Kobe, S. Photoinduced Properties of Nanocrystalline TiO_2-Anatase Coating on Ti-based Bone Implants. *Mater. Sci. Eng., C* **2014**, *37*, 390−398.
(7) Wu, H.; Wang, L. Electronic Structure of Titanium Oxide Clusters: TiOy (y=1−3) and (TiO_2)n (n=1−4). *J. Chem. Phys.* **1997**, *107*, 8221−8228.
(8) Binetti, E.; Panniello, A.; Agostiano, A.; Fantini, S.; Curri, M. L.; Striccoli, M. Interaction of TiO_2 Nanocrystals with Imidazolium-Based Ionic Liquids. *J. Phys. Chem. C* **2013**, *117*, 12923−12929.
(9) Wittmar, A.; Ulbricht, M. Dispersions of Various Titania Nanoparticles in Two Different Ionic Liquids. *Ind. Eng. Chem. Res.* **2012**, *51*, 8425−8433.
(10) Rønnau, A. A. Closer Look at the TiO_2 (110) Surface with STM. Ph.D. Thesis. University of Aarhus, Aarhus, Denmark, 2003.
(11) Martins, M. A. P.; Frizzo, C. P.; Moreira, D. N.; Zanatta, N.; Bonacorso, H. G. Ionic Liquids in Heterocyclic Synthesis. *Chem. Rev.* **2008**, *108*, 2015−2050.
(12) Brown, P.; Butts, C. P.; Eastoe, J.; Fermin, D.; Grillo, I.; Lee, H.; Parker, D.; Plana, D.; Richardson, R. M. Anionic Surfactant Ionic Liquids with 1-Butyl-3-Methyl-Imidazolium Cations: Characterization and Application. *Langmuir* **2012**, *28*, 2502−2509.
(13) Minami, I. Ionic Liquids in Tribology. *Molecules* **2009**, *14*, 2286−2305.
(14) Preocanin, T.; Kallay, N. Point of Zero Charge and Surface Charge Density of TiO_2 in Aqueous Electrolyte Solution as Obtained by Potentiometric Mass Titration. *Croat. Chem. Acta* **2006**, *79*, 95−106.
(15) Monti, S.; Carravetta, V.; Battocchio, C.; Iucci, G.; Polzonetti, G. Peptide/TiO_2 Surface Interaction: A Theoretical and Experimental Study on the Structure of Adsorbed ALA-GLU and ALA-LYS. *Langmiur* **2008**, *13*, 3205−3214.
(16) Vallee, A.; Humblot, V.; Pradier, C.-M. Peptide Interactions with Metal and Oxide Surfaces. *Acc. Chem. Res.* **2010**, *43*, 1297−1306.
(17) Wang, S.; Cao, Z.; Li, S.; Yan, T. A Molecular Dynamics Simulation of the Structure of Ionic Liquid (BMIM+/PF6−)/rutile (110) Interface. *Sci. China Ser. B: Chem.* **2009**, *52*, 1434−1437.
(18) Chen, X.; Li, Q.; Zhao, J.; Qiu, L.; Zhang, Y.; Sun, B.; Yan. Ionic Liquid-Tethered Nanoparticle/Poly(Ionic Liquid) Electrolytes for Quasi-Solid-State Dye-Sensitized Solar Cells. *J. Power Sources* **2012**, *207*, 216−222.
(19) Zhou, F.; Liang, Y.; Liu, W. Ionic Liquid Lubricants: Designed Chemistry for Engineering Applications. *Chem. Soc. Rev.* **2009**, *38*, 2590−2599.
(20) Jiménez, A. E.; Bermúdez, M. D. Ionic Liquids as Lubricants of Titanium−Steel Contact. Part 2: Friction, Wear and Surface Interactions at High Temperature. *Tribol. Lett.* **2009**, *37*, 431−443.
(21) Han, C.-C.; Ho, S.-Y.; Lin, Y.-P.; Lai, Y.-C.; Liang, W.-C.; Chen-Yang, Y.-W. Effect of $\pi-\pi$ Stacking of Water Miscible Ionic Liquid Template with Different Cation Chain Length and Content on Morphology of Mesoporous TiO_2 Prepared via Sol−Gel Method and the Applications. *Microporous Mesoporous Mater.* **2010**, *131*, 217−223.
(22) Suzuki, S.; Ohta, Y.; Kurimoto, T.; Kuwabata, S.; Torimoto, T. Modulating the Immobilization Process of Au Nanoparticles on TiO_2(110) by Electrostatic Interaction Between the Surface and Ionic Liquids. *Phys. Chem. Chem. Phys.* **2011**, *13*, 13585−13593.
(23) Kislenko, S. A.; Amirov, R. H.; Samoylov, I. S. Effect of Cations on the TiO_2/Acetonitrile Interface Structure: A Molecular Dynamics Study. *J. Phys. Chem. C* **2013**, *117*, 10589−10596.
(24) Chang, H.; Chang, S.; Hung, T.; Jiang, J.; Kuo, J.; Lin, S. H. A High-Pressure Study of the Effects of TiO_2 Nanoparticles on the Structural Organization of Ionic Liquids. *J. Phys. Chem. C* **2011**, *115*, 23778−23783.
(25) Wittmar, A.; Gajda, M.; Gautam, D.; Dörfler, U.; Winterer, M.; Ulbricht, M. Influence of the Cation Alkyl Chain Length of Imidazolium-Based Room Temperature Ionic Liquids on the Dispersibility of TiO_2 Nanopowders. *J. Nanopart. Res.* **2013**, *15*, 1463.
(26) Alammar, T.; Noei, H.; Wang, Y.; Mudring, A.-V. Mild Yet Phase-Selective Preparation of TiO_2 Nanoparticles from Ionic Liquids - A Critical Study. *Nanoscale* **2013**, *5*, 8045−8055.
(27) Tkachenko, N. H.; Yaremko, Z. M.; Bellmann, C. Effect of 1−1-Charged Ions on Aggregative Stability and Electrical Surface Properties of Aqueous Suspensions of Titanium Dioxide. *Colloids Surf., A* **2006**, *279*, 10−19.
(28) Hayes, R.; Borisenko, N.; Tam, M. K.; Howlett, P. C.; Endres, F.; Atkin, R. Double Layer Structure of Ionic Liquids at the Au(111) Electrode Interface: An Atomic Force Microscopy Investigation. *J. Phys. Chem. C* **2011**, *115*, 6855−6863.
(29) Bermúdez, M.-D.; Jiménez, A.-E.; Sanes, J.; Carrión, F.-J. Ionic Liquids as Advanced Lubricant Fluids. *Molecules* **2009**, *14*, 2888−2908.
(30) Martins, M. A. P.; Guarda, E. A.; Frizzo, C. P.; Moreira, D. N.; Marzari, M. R. B.; Zanatta, N.; Bonacorso, H. G. Ionic Liquids Promoted the C-Acylation of Acetals in Solvent-free Conditions. *Catal. Lett.* **2009**, *130*, 93−99.
(31) Shirota, H.; Mandai, T.; Fukazawa, H.; Kato, T. Comparison between Dicationic and Monocationic Ionic Liquids: Liquid Density, Thermal Properties, Surface Tension, and Shear Viscosity. *J. Chem. Eng. Data* **2011**, *56*, 2453−2459.
(32) Rodrigues, D. C.; Bader, R. A.; Hasenwinkel, J. M. Grafting of Nanospherical PMMA Brushes on Cross-linked PMMA Nanospheres for Addition in Two-solution Bone Cements. *Polymer* **2011**, *52*, 2505−2513.
(33) Frizzo, C. P.; Villetti, M. A.; Tier, A. Z.; Gindri, I. M.; Buriol, L.; Rosa, F. A.; Claramunt, D. S.; Martins, M. A. P. Structural and Thermodynamic Properties of New Pyrazolo[3,4-d]pyridazinones. *Thermochim. Acta* **2013**, *574*, 63−72.
(34) Bertasi, F.; Vezzù, K.; Negro, E.; Greenbaum, S.; Di Noto, V. Single-Ion-Conducting Nanocomposite Polymer Electrolytes Based on PEG400 and Anionic Nanoparticles: Part 1. Synthesis, Structure and Properties. *Int. J. Hydrogen Energy* **2014**, *39*, 2872−2883.
(35) Xue, J.-J.; Chen, Q.-Y. The Interaction Between Ionic Liquids Modified Magnetic Nanoparticles and Bovine Serum Albumin And the Cytotoxicity to HepG-2 Cells. *Spectrochim. Acta, Part A* **2014**, *120*, 161−166.
(36) Vangala, V. R.; Chow, P. S.; Tan, R. B. H. Co-Crystals and Co-Crystal Hydrates of the Antibiotic Nitrofurantoin: Structural Studies and Physicochemical Properties. *Cryst. Growth Des.* **2012**, *12*, 5925−5938.
(37) Shen, J. P.; Duan, X. H.; Luo, Q. P.; Zhou, Y.; Bao, Q.; Ma, Y. J.; Pei, C. H. Preparation and Characterization of a Novel Cocrystal Explosive. *Cryst. Growth Des.* **2011**, *11*, 1759−1765.
(38) Praus, P.; Dvorský, R.; Horínková, P.; Pospíšil, M.; Kovář, P. Precipitation, Stabilization and Molecular Modeling of ZnS Nanoparticles in the Presence of Cetyltrimethylammonium Bromide. *J. Colloid Interface Sci.* **2012**, *377*, 58−63.
(39) Chen, T.; Cao, Z.; Guo, X.; Nie, J.; Xu, J.; Fan, Z.; Du, B. Preparation and Characterization of Thermosensitive Organic−Inorganic Hybrid Microgels with Functional Fe3O4 Nanoparticles as Crosslinker. *Polymer* **2011**, *52*, 172−179.

(40) Liu, X. Y.; Zheng, S. W.; Hong, R. Y.; Wang, Y. Q.; Feng, W. G. Preparation of Magnetic Poly(styrene-co-acrylic acid) Microspheres with Adsorption of Protein. *Colloids Surf., A* **2014**, *443*, 425−431.
(41) Villetti, M. A.; Borsali, R.; Crespo, J. S.; Soldi, V.; Fukada, K. Static and Dynamic Light Scattering of Polyelectrolyte/Surfactant Solutions: The Na-Hyaluronate/(C10TAB) System. *Macromol. Chem. Phys.* **2004**, *205*, 907−917.
(42) Chen, Y.; Ke, F.; Wang, H.; Zhang, Y.; Liang, D. Phase Separation in Mixtures of Ionic Liquids and Water. *ChemPhysChem* **2012**, *13*, 160−167.
(43) Mamani, J. B.; Costa-Filho, A. J.; Cornejo, D. R.; Vieira, E. D.; Gamarra, L. F. Synthesis and Characterization of Magnetite Nanoparticles Coated with Lauric Acid. *Mater. Charact.* **2013**, *81*, 28−36.
(44) Al-kaysi, R. O.; Mu, A. M.; Frisbee, R. J.; Bardeen, C. J. Formation of Cocrystal Nanorods by Solid-State Reaction of Tetracyanobenzene in 9-Methylanthracene Molecular Crystal Nanorods. *Cryst. Growth Des.* **2009**, *9*, 1781−1785.
(45) Mulye, S. P.; Jamadar, S. A.; Karekar, P. S.; Pore, Y. V.; Dhawale, S. C. Improvement in Physicochemical Properties of Ezetimibe Using a Crystal Engineering Technique. *Powder Technol.* **2012**, *222*, 131−138.
(46) Jung, Y.; Choi, J.; Oh, J.-W.; Kim, N. Synthesis of Uniform Hollow Poly(N-vinylcarbazole) and Liquid Crystal/poly(N-vinylcarbazole) Core/Shell Nanoparticles. *Synth. Met.* **2013**, *163*, 24−28.